Supporting Information

Dehydration of Gypsum Waste to Recyclable Anhydrite Using a Nano-Film Reservoir under Ambient Conditions

Chunli Wang[1,2], Wenjing Li[1], Chunli Gou[1], Zhihao Zhang[1], Zhang Lin*[1,2], *Jing Zhang*[1]*

1 Research Center for Environmental Material and Pollution Control Technology, University of Chinese Academy of Sciences, Beijing 101408, P. R. China

[2] Chinese National Engineering Research Centre for Control & Treatment of Heavy Metal Pollution, School of Metallurgy and Environment, Central South University, Changsha 410083, China

Contents

Supplementary Discussion

Calculation of phase diagrams.

As shown in Fig. 4a, the free energy difference *(*ΔG) was described as a function of water activity and temperature and can be written as:

$$\Delta G = G_a + G_w - G_g \#(1-1)$$

where G_g, G_a, and G_w are the free energy of gypsum, anhydrite, and water, respectively. Specifically, at atmospheric pressure， G_g and G_a are considered approximately dependent on temperature, while G_w is determined by both temperature and vapor pressure. The G_g and G_a were obtained within the QHA by calculating the phonon states as a function of temperature (Figure S5). The G_w value is obtained by correcting the free energy of a single water molecule at temperature (T) and pressure (P) of the phase diagram. The abscissa of the phase diagram is the water activity, which can be described by P/P_0. P_0 is the vapor pressure of pure water at the corresponding temperature. Furthermore, to understand the energy landscape in the calcium sulfate system in NSF, we initially determined the transformation of free energy between gypsum and anhydrite with the reaction heats calculated from the standard formation enthalpies at 300 K[1]:

$$CaSO_4 \cdot 2H_2O_{(s)} \rightarrow CaSO_{4(s)} + 2H_2O_{(g)} \#\Delta G = 41\ kJ/mol \quad (1-2)$$

Thus, a change in ΔG of 41 kJ/mol explains the transformation is thermodynamically prohibited under ambient conditions.

Kinetic model

To structurally monitor the evolution of gypsum, we employed in-situ X-ray diffraction for the dehydration in the water reservoir (see tracking of the phase transformation in the experimental section). Figure S6a. shows that the gypsum peaks

disappeared rapidly before the formation of bassanite at 5 min, and then the immediate phase γ-$CaSO_4$ convert into anhydrite after 650 min. A slight shift of all the bassanite peaks to a lower angle at 5 to 10 min proves the formation of γ-$CaSO_4$, which has almost the same structure as bassanite except crystal water free[2]. This result reveals that the structural transition from γ-$CaSO_4$ to anhydrite kinetically limits the anhydrite formation.

On the contrary, the gypsum disappeared slowly for 200 min in NSF at 323 K, indicating that complete dehydration to form anhydrite skipped the γ-$CaSO_4$ (Figure S7a.). The anhydrite peak located at 2θ = 25.5° gradually emerges after 25 minutes, is accompanied by a set of simultaneous bassanite peaks, which are relatively weak and not durable. We extrapolate that these transitional bassanites formed at 323 K arise from the partial dehydration of gypsum triggered by heating because they are also observed in absence of NSF at the same temperature. Combined with the literature that a considerable amount of time (e.g. 2 years at 60 °C) is needed for anhydrite to form[3], our findings confirmed that NSF dramatically accelerated dehydration to form anhydrite. On a qualitative level, this acceleration may be explained by a different pathway for the dehydration-induced structural transformation based on the above time-resolved XRD observations, that is, a faster route for anhydrite formation may be triggered by the NSF rather than just quickening the rate of the traditional reaction.

Our kinetic model assumes that the conversion of gypsum to anhydrite occurs only in nucleation and growth, and describes the changes in the conversion rate ($\alpha(t)$) via time integrals of nuclei and growth volume. According to this model, we get the nucleation rate and the flux for growth by fitting the time series conversion rate $\alpha(t)$ in Figure S8. The result derived in this paper is the following equality:

$$\alpha(t) = \frac{\left(J\sigma e^{t\left(J\sigma - V_s\varepsilon\tau\right)} - V_s\varepsilon\tau e^{t_m\left(J\sigma - V_s\varepsilon\tau\right)}\right)e^{-t_m\left(J\sigma - V_s\varepsilon\tau\right)}}{J\sigma - V_s\varepsilon\tau} \#(2-1)$$

Before proceeding with the proof of Eq. (2-1), we establish notation and then relate Eq. (2-1) to the nucleation and growth. Let V_e denote the volume of anhydrite after complete dehydration, and the volume at time t is $\alpha(t)V_e=V_n(t)+V_g(t)$, where $V_n(t)$ is the nuclei volume accumulated up to time t and $V_g(t)$ is the volume obtained due to the growth of these nuclei. Let τ be the nucleation rate, the number of nuclei formed per gypsum volume per unit time. Thus, $V_n(t)$ can be described by the time integral of $V_s \cdot \tau \cdot V_r(t)$, where V_s is the volume of a single nucleus, τ is nucleation rate and $V_r(t)$ is the residual volume of gypsum at time t. Since the molar amount of $CaSO_4$ is conserved during the phase transition, $V_r(t)$ is equal to the change of $\varepsilon(1-\alpha(t))V_e$, where ε is the molar volume ratio of gypsum and anhydrite. Therefore, we get:

$$V_n(t) = \int_0^t V_s \tau \varepsilon (1 - \alpha(t)) V_e dt \#(2-2)$$

Since the as-formed nuclei with different sizes have been observed, suggesting that the particle growth caused by Ostwald maturation is not significant, we explicitly assume the specific surface area (σ) is constant in anhydrite that has been formed. Here σ was determined by BET as 0.7787 m^2/g. Therefore, $V_g(t)$ is just the growth volume accumulated up to time t and may be expressed as:

$$V_g(t) = \int_0^t J \sigma \alpha(t) V_e dt \#(2-3)$$

Now, the volume add to anhydrite by growth is equal to the volume flux J accumulation along time and surface. Combining formular (2-2) gives

$$\alpha(t)V_e = \int_0^t V_s \tau \varepsilon (1 - \alpha(t)) V_e dt + \int_0^t J \sigma \alpha(t) V_e dt \#(2-4)$$

Considering the boundary condition, $\alpha(t)=1$ at $t = t_{max}$, solving differential equation (2-4), then we gives

$$J = -\frac{W\left(-V_n t_m \varepsilon \tau e^{-V_n t_m \varepsilon \tau}\right)}{t_m \sigma} \#(2-5)$$

where the W means the Lambert W function. Therefore, the flux is determined by the nucleation rate τ and the time t_{max} when a phase transformation is expected to be completed. We have calculated the value of J at different temperature in Fig 4c insert.

In addition, the constant k_i describes the induction period ($\alpha(t)$<0.01) of the conversion, modeled with zero order kinetics, because the concentration of the reactant in the induction period, that is, the solubility of gypsum, is constant as a pure phase[4].

$$\frac{d\alpha}{dt} = k_i(\alpha \leq 0.01) \#(2-6)$$

In the classical view of crystallization, the number of nuclei formed per volume per unit time, nucleation rate τ, describes the rate of nucleation. τ is associated with the energy barriers of desolvation (ΔU) and crystallization (ΔG)[4]. It follows that

$$\tau = 4\pi r^2 C^2 \upsilon \lambda exp\left(-\frac{\Delta U}{RT}\right) \Gamma exp\left(-\frac{\Delta G}{RT}\right) \#(2-7)$$

Regarding the formation of nuclei with a radius of r in solution with concentration C, the frequency factor ν depend on the temperature, the mean free path of ions λ and Zeldovich Γ[5], which can be written as:

$$\Gamma = \left(\frac{\Delta G}{3\pi RT r^2}\right)^{\frac{1}{2}} \#(2-8)$$

To eliminate errors brought by estimating r, C, v, λ, and Γ, setting $4\pi r^2 C^2 v \lambda \Gamma = A$ and $\Delta U + \Delta G = E$ in the equation above gives

$$\tau = A e^{\frac{-E}{RT}} \#(2-9)$$

Through formular 2-9, the E have been obtained by fitting τ at different temperatures in Figure S9.

Supplementary Figures

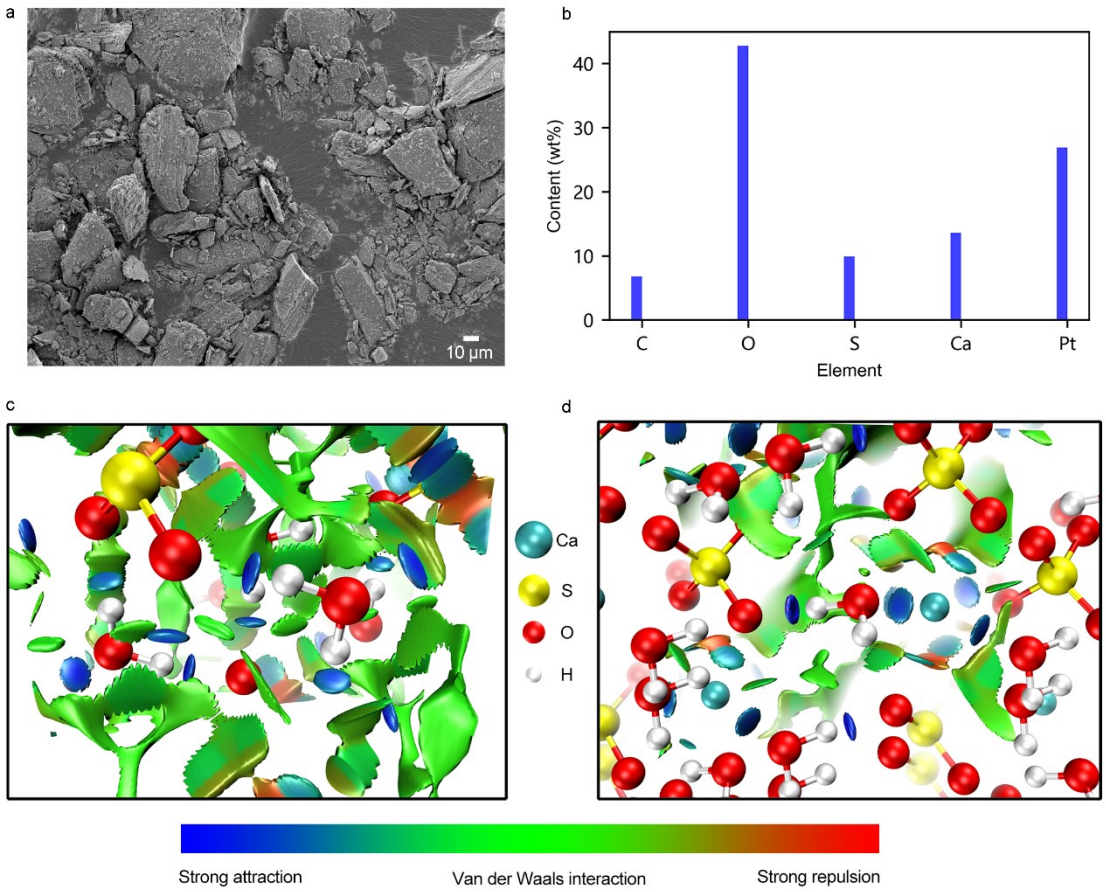

Figure S1. (a, b), Scanning electron microscope (SEM) photos and energy dispersive spectroscopy (EDS) elemental analysis of gypsum samples. (c, d) NCI interaction regions for gypsum (c) and the interface of gypsum-NSF(d).

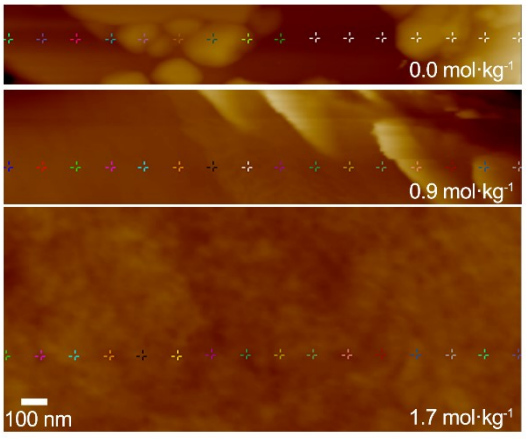

Figure S2. AFM height image of anhydrite at various initial sulfuric acid concentrations.

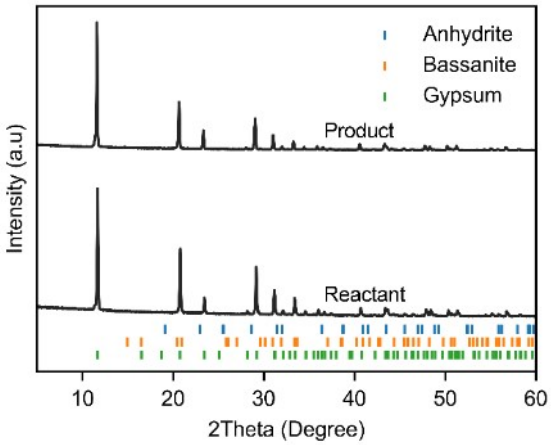

Figure S3. XRD patterns of the reactant and the product after adding 0.9 mol·kg^{-1} sulfuric acid solution at 300 K for 7 days.

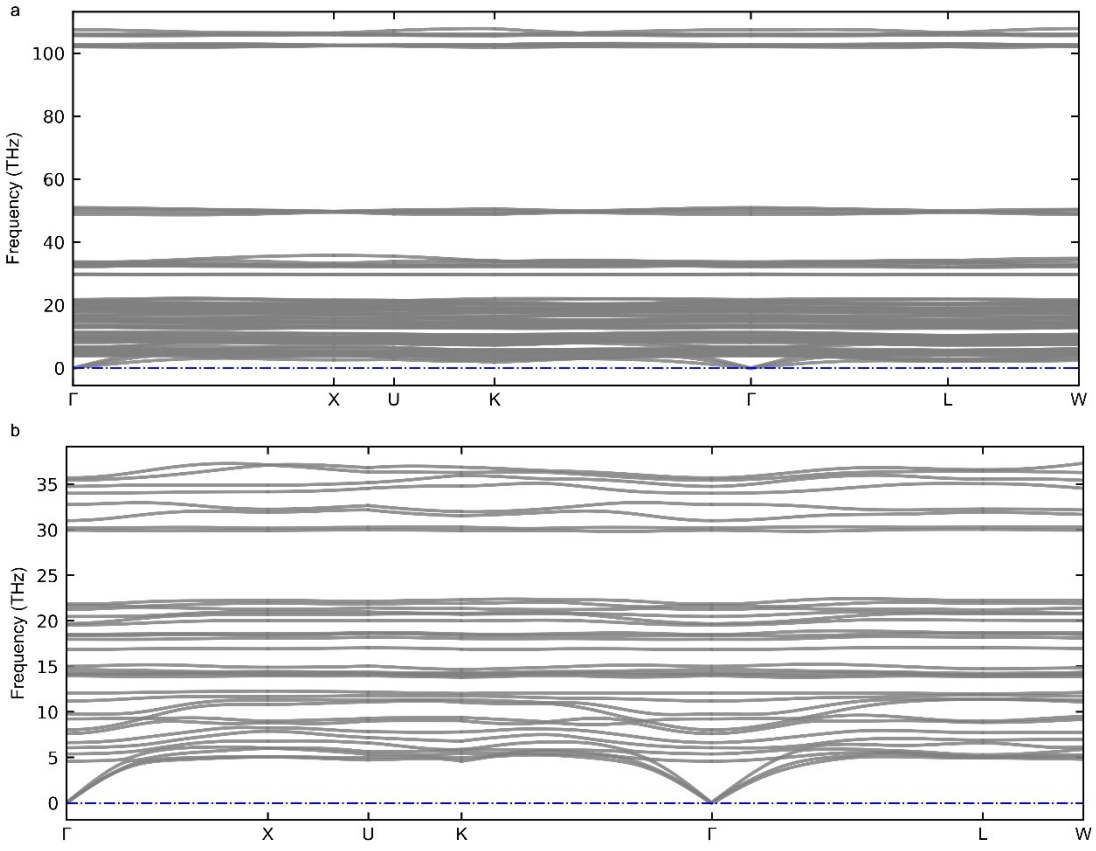

Figure S4. Phonon band structures of gypsum (a) and anhydrite (b).

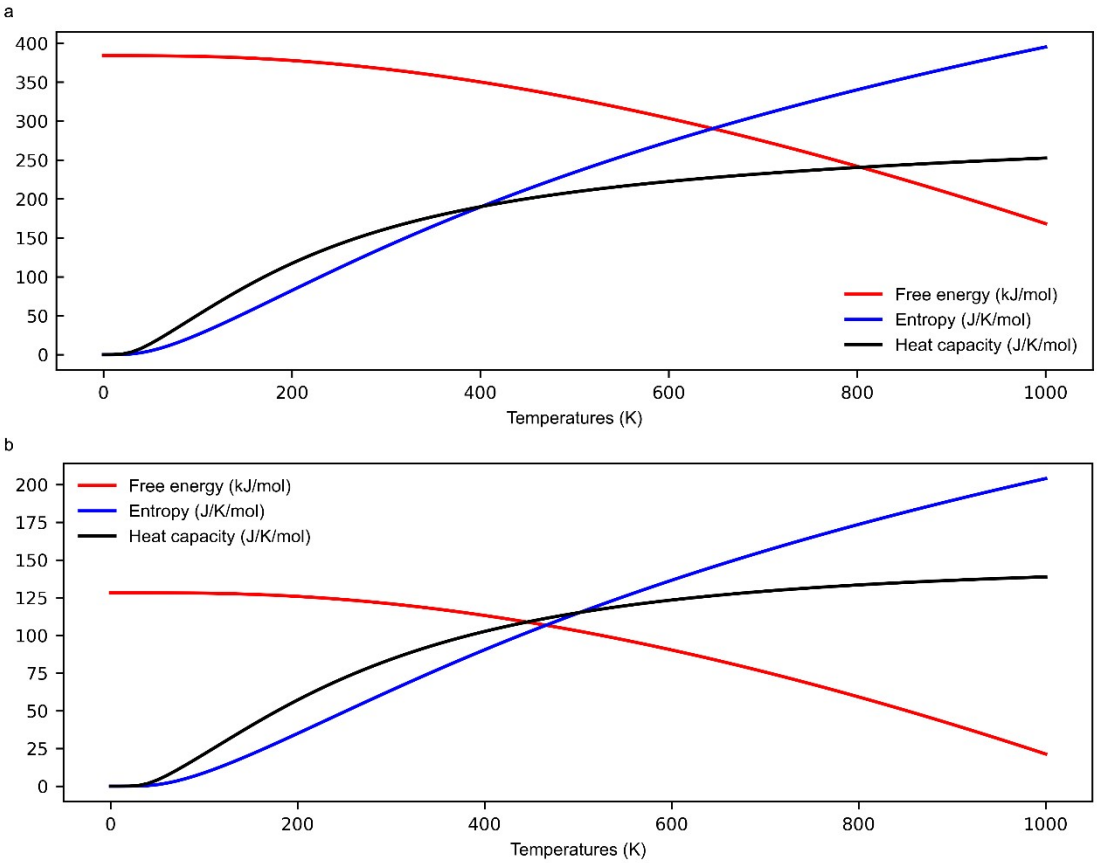

Figure S5. Thermodynamic properties at different temperatures for gypsum (a) and anhydrite (b).

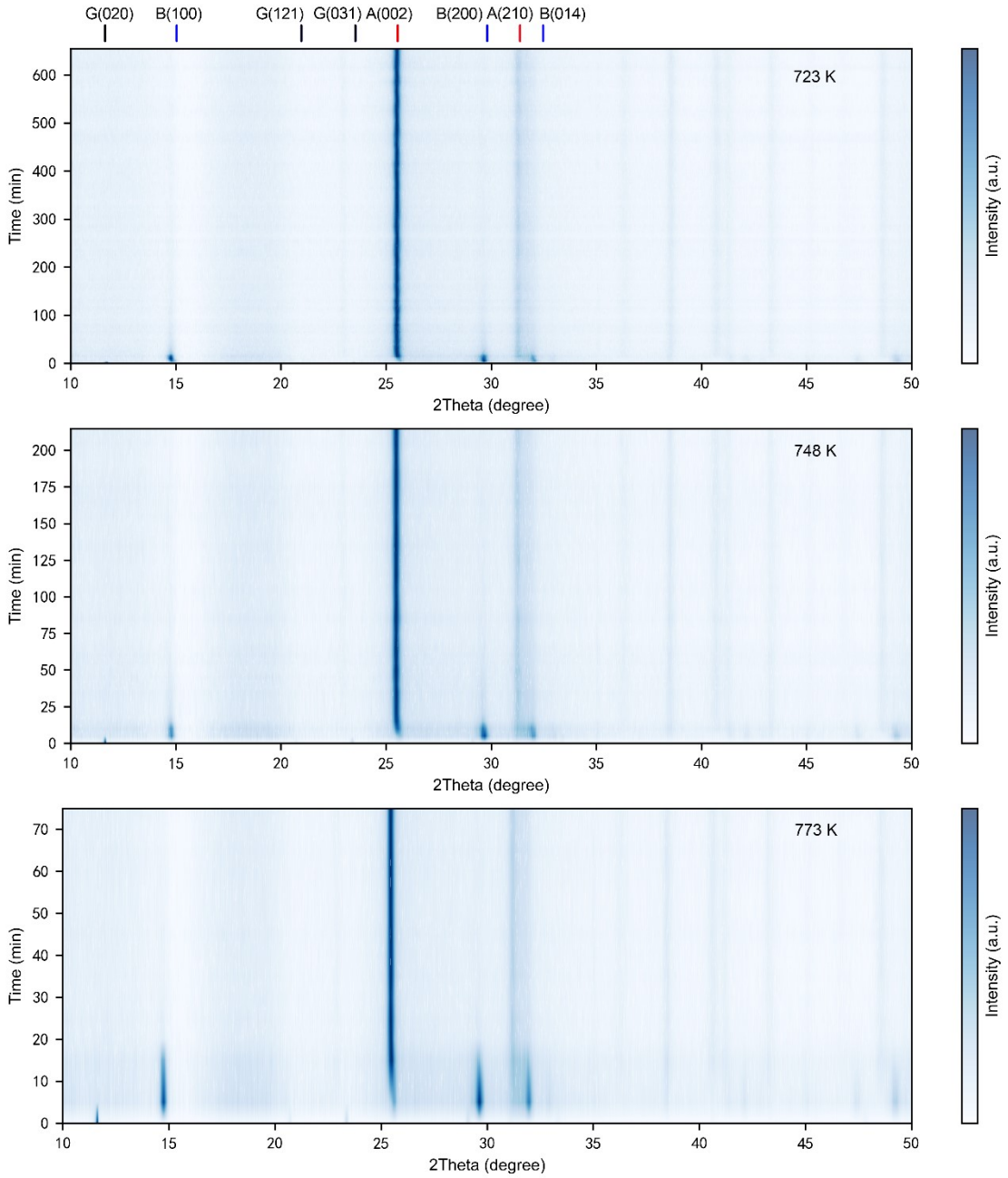

Figure S6. In-situ X-ray diffraction model collected by heating gypsum without NSF at 723 K **(a)**, 748 K**(b)** and 773 K**(c)**. The vertical solid lines at the top are a guide to the eye for distinguishing the gypsum (black), bassanite (blue), and anhydrite (red) conveniently.

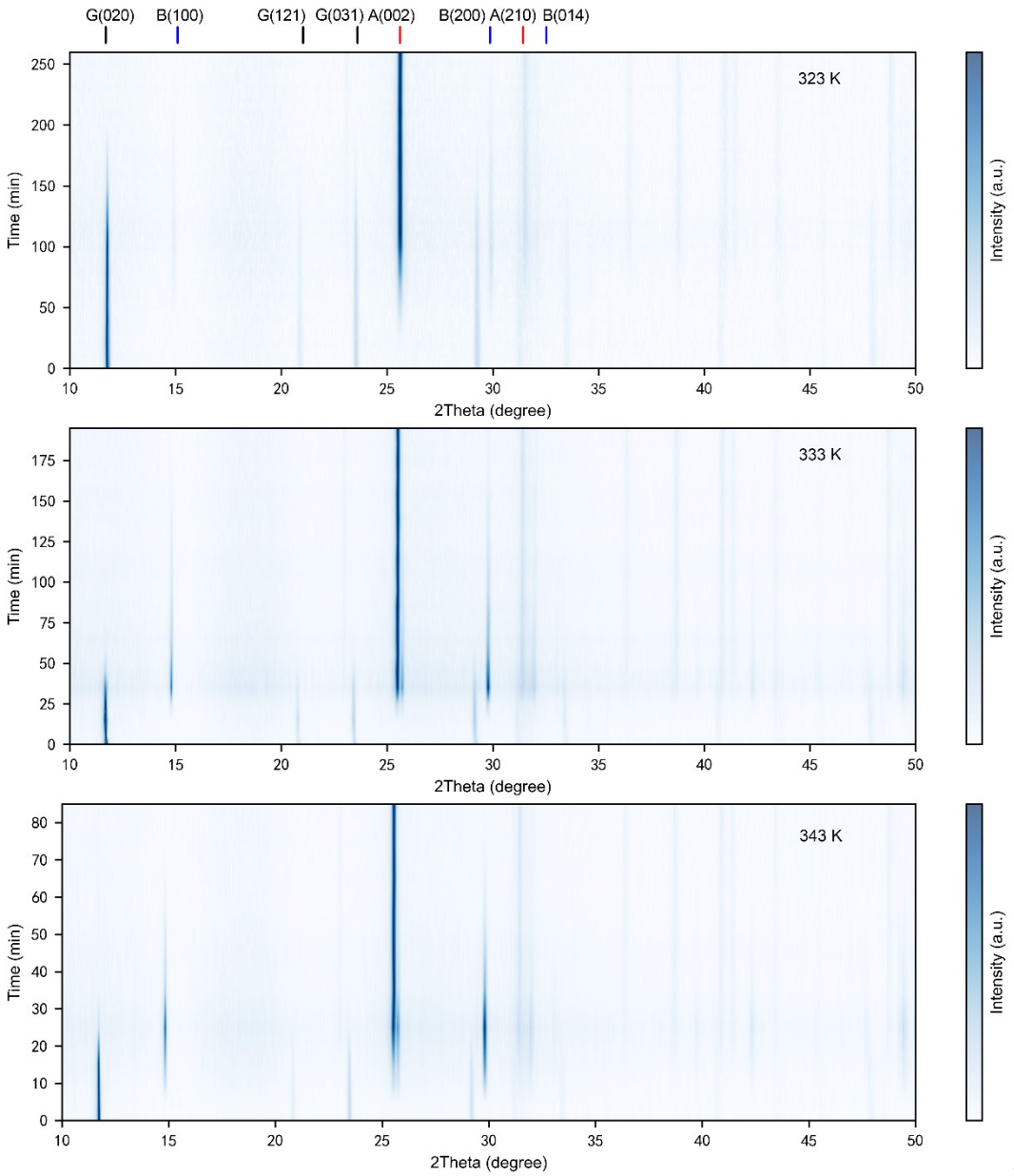

Figure S7. In-situ X-ray diffraction model collected by heating gypsum in NSF at 323 K **(a)**, 333 K**(b)** and 343 K**(c)**. The vertical solid lines at the top are a guide to the eye for distinguishing the gypsum (black), bassanite (blue), and anhydrite (red) conveniently.

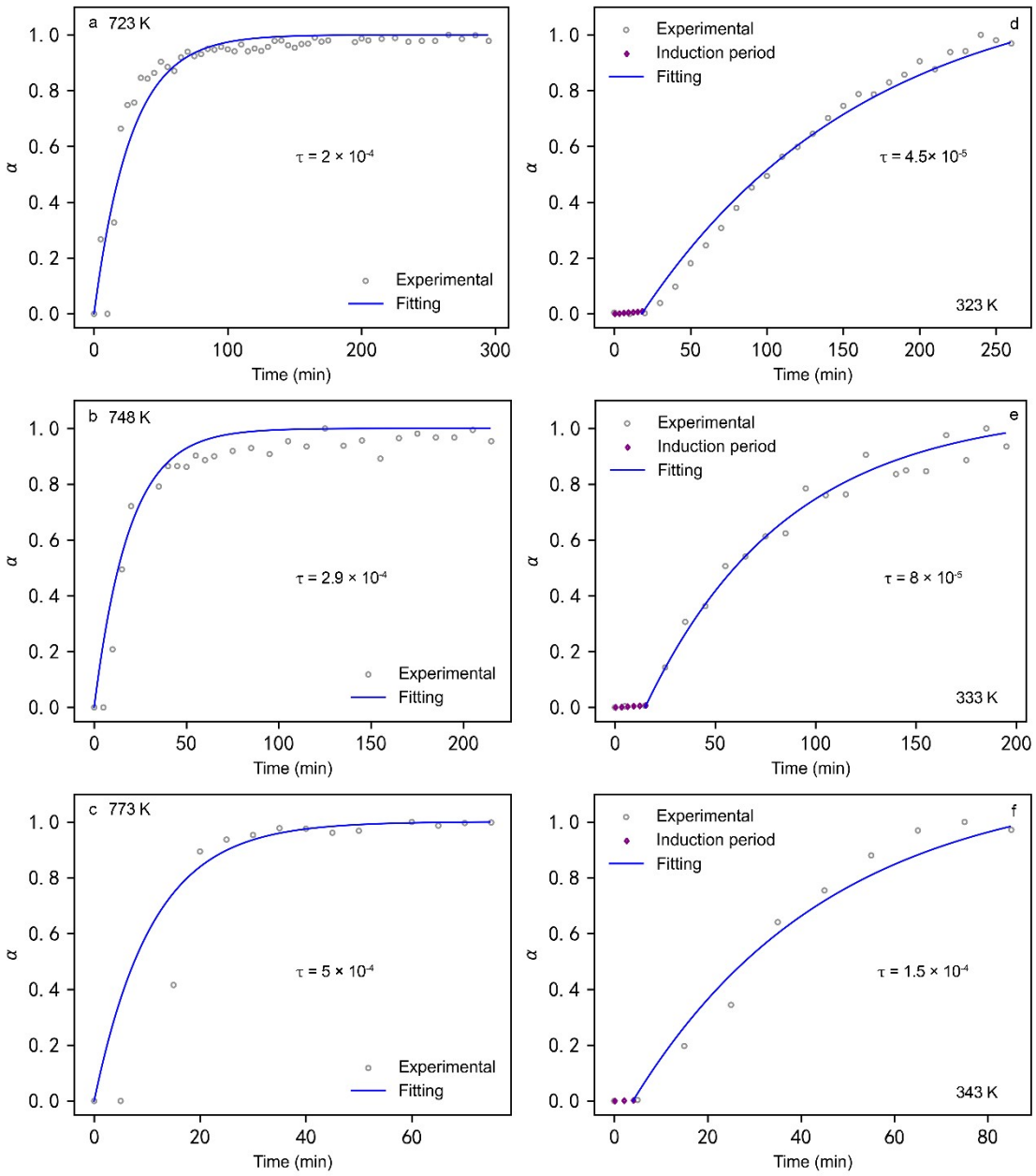

Figure S8. Phase-conversion kinetics. We investigate that the nucleation rate of τ effect the conversion rate (α(t)) with the further heating time either in absence of NSF at 723 K**(a)**, 748 K**(b)** and 773K **(c)** or in NSF at 323 K**(d)**, 333 K**(e)** and 343 K **(f)**. When we investigate the value of τ, the value of k_0 is taken as the best fitting value, which corresponds to the purple scatter in the **(d-f)**.

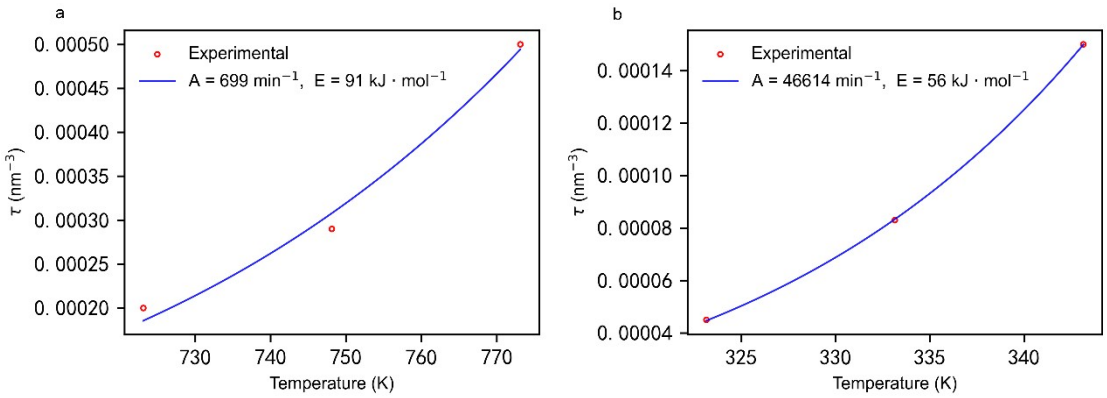

Figure S9. Results of fitting nucleation rate using formula (2-9).

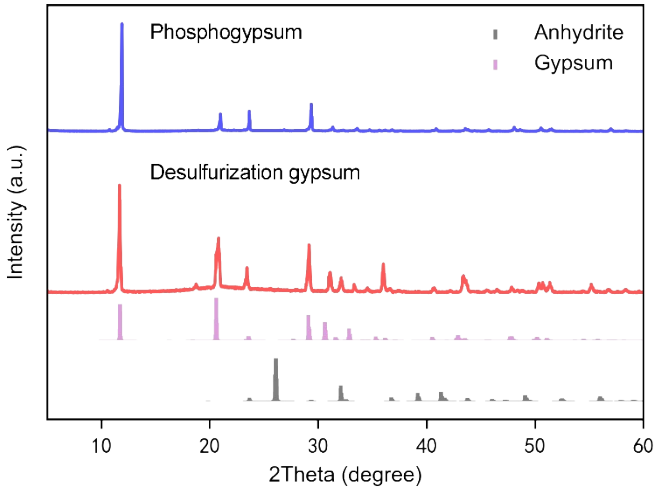

Figure S10. XRD patterns of the phosphogypsum and desulfurization gypsum samples.

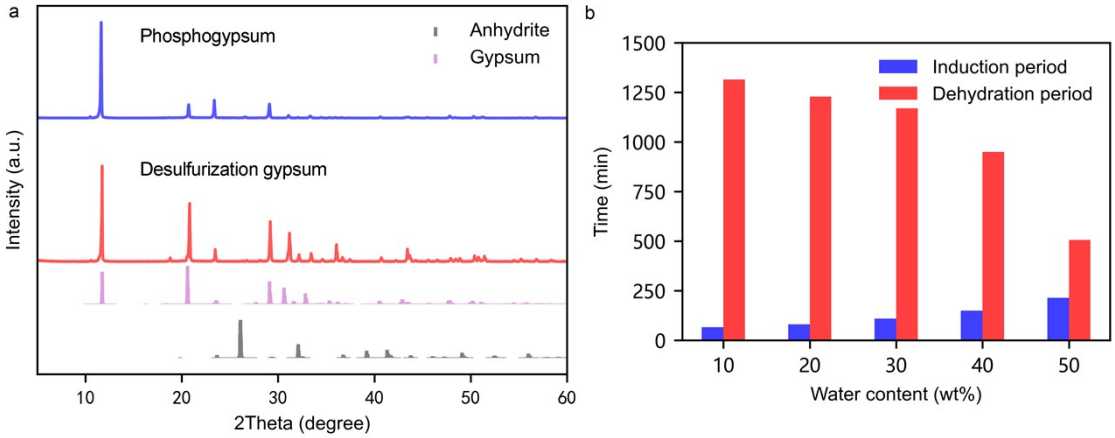

Figure S11. (a) XRD patterns of the phosphogypsum and desulfurization gypsum samples dried at 40 ℃ for three days. (b) Time consumed in dehydration of varying water contents gypsum

employing the NSF. The induction period pertains to the interval commencing from the introduction of sulfuric acid solution to the onset of formation of anhydrite, while the dehydration period signifies the temporal span encompassing the emergence of anhydrite to the eventual dissipation of gypsum.

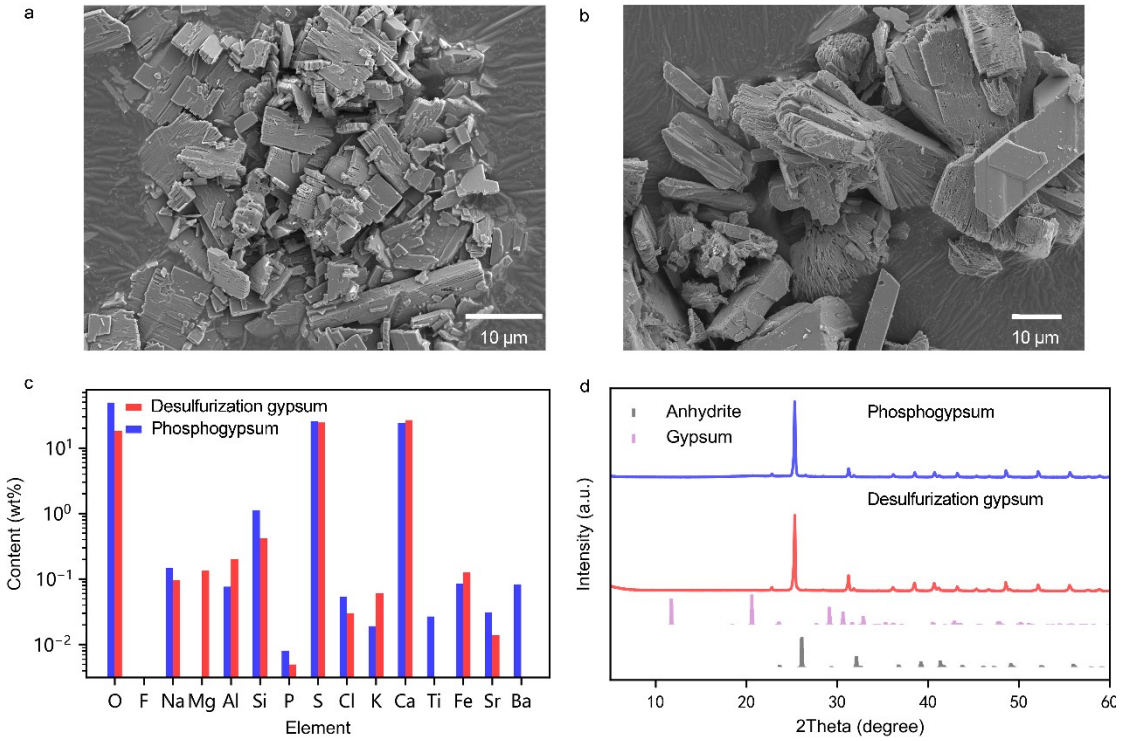

Figure S12. (a, b), Scanning electron microscope (SEM) photos of phosphogypsum (a) and desulfurization gypsum (b) after dehydration. (c, d), XRF quantification of elements (c) in anhydrites produced from phosphogypsum and desulfurization gypsum and their XRD patterns (d).

Reference

1.Linstrom PJ, Mallard WG, WebBook NC, NIST Standard Reference Database Number 69 =, Gaithersburg MD, 20899.

2.Lager GA, Armbruster T, Rotella FJ, Jorgensen JD, Hinks DG. A crystallographic study of the low-temperature dehydration products of gypsum, $CaSO_4 \cdot 2H_2O$: hemihydrate, $CaSO_4 \cdot 0.50H_2O$, and γ-$CaSO_4$. *American Mineralogist* **1984**, 69, 910-919.

3.Ossorio M, Van Driessche AES, Perez P, Garcia-Ruiz JM. The gypsum-anhydrite paradox revisited. *Chem. Geol.* **2014**, 386, 16-21.

4.Walton G. Nucleation in liquid and solution. *Nucleation* **1969**, 606.

5.Zeldovich J. Acta physicochim. *URSS* **1946**, 21, 577.